THE JOURNAL OF PHYSICAL CHEMISTRY C

Article

pubs.acs.org/JPCC

Effect of Electric Field on Condensed-Phase Molecular Systems. I. Dipolar Polarization of Amorphous Solid Acetone

Sunghwan Shin, Youngsoon Kim, Hani Kang, and Heon Kang*

Department of Chemistry, Seoul National University, 1 Gwanak-ro, Seoul 151-747, South Korea

ABSTRACT: We investigated the dipolar reorientation of acetone molecules in amorphous solids under the influence of externally applied electric fields in the range of $(0-4.3) \times 10^8$ V·m^{-1}. The electric field was applied using an ice film capacitor method, and the field strength was estimated from measurements of the film voltage and thickness using a Kelvin probe and the temperature-programed desorption method, respectively. Reorientation of the acetone molecules was monitored with reflection−absorption infrared spectroscopy (RAIRS), which measured the absorbance change of the acetone vibrational bands induced by the applied electric field. The electric field caused a substantial degree of dipolar polarization of the sample. Acetone molecules were reoriented toward the field direction by an average angle of about 31° at an applied field strength of 4.3×10^8 V·m^{-1}, according to analysis of the RAIRS intensity changes using a simple molecular geometry model. While the extent of dipolar polarization of the sample increased with increasing field strength, the sample was not reversibly depolarized with decreasing field strength. Multiple-peak analysis of the ν(C═O) spectrum revealed that the molecules in the acetone−water boundary region were more easily rotated compared to those in the bulk.

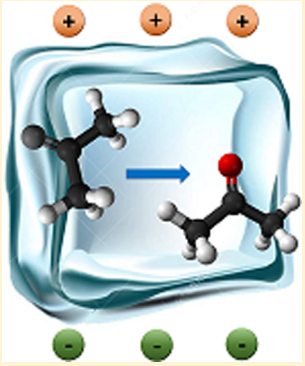

1. INTRODUCTION

Strong electric fields routinely exist in the local environment of molecules in the condensed phase, for example, near ionized groups or permanent dipoles of molecules and within the electrical double layers formed at solid/solution interfaces. The local electric fields can have a profound influence on the intermolecular interactions and reactions of molecules. There are numerous such examples, including the reorientation of solvent molecules induced by electric field.[1] In the 1970s, Simons[2,3] observed significant enhancement in ionic current due to proton transfer between water and surface-bound amines of ion-exchange membranes, and claimed that these processes are facilitated by the alignment of water molecules under the influence of strong electric fields at the membranes and/or the dissociation of weak acids and bases in the so-called second Wien effect.[4] Toney et al.[5] studied the interfacial structure of water at an Ag(111) electrode surface by means of in situ X-ray scattering techniques, and reported potential-dependent reorientation of the water molecules adsorbed on the surface. Although certain aspects of the reported water structure are disputable, it is generally agreed that water flipping can occur in the presence of strong electric fields at electrode/solution interfaces.[6,7] Electric field also plays an essential role in determining protein functions, such as folding, molecular recognition, and catalytic reactions, under physiological conditions.[8,9] In the early studies, however, the electric fields present at the electrode or protein surfaces were not well characterized. It is highly desirable to perform experiments under well-defined field conditions for systematically studying the effects of electric field on molecular behavior.

To study the reorientation of polar solvents induced by electric field, a strong field with a magnitude of $\sim 10^8$ V·m^{-1} is required. This magnitude is comparable to the field strength observed near charged species in solutions. Various experimental methods have been devised to generate and utilize strong electric fields for investigating their effects on molecules in condensed phases. These methods include the use of charged parallel metal plates,[10−12] electrical double layers,[6,13] field ionization tips,[14] and charging of molecular films with ion[15,16] or electron deposition.[17] Each of these methods have their own advantages and limitations, depending on the applications for which they are used.[18] Strong fields cause several practical problems, such as dielectric breakdown of liquid samples and the generation of ionic currents in the case of electrolyte solutions. These limitations can be significantly reduced by using glassy samples. Boxer and co-workers[10,11] pioneered this approach and showed that electric fields with strengths of the order of 10^8 V·m^{-1} can be applied across thin films of frozen molecular solids by using charged parallel metal plates. At present, progress in research on electric field effects on molecular behavior is closely tied to the development of technology for generating strong electric fields applicable to molecular systems.

Recently, Shin et al.[18] reported an ice film capacitor method that can be used to apply strong electric fields across frozen molecular films. In this method, a sample is charged by trapping Cs^+ ions at the surface of an ice overlayer on the sample via thermodynamic forces, without using parallel metal plates. This method possesses several advantages over conventional methods, including the ability to generate stronger electric fields ($\sim 4 \times 10^8$ V·m^{-1}) compared to a metal plate capacitor, ability to control the sample composition and structure in a

Received: February 24, 2015
Revised: May 15, 2015
Published: May 19, 2015

DOI: 10.1021/acs.jpcc.5b01849
J. Phys. Chem. C 2015, 119, 15588−15595

clean vacuum environment, and compatibility with in situ surface spectroscopy methods to facilitate direct monitoring of the sample under applied electric field. In the present work, we use this method to study the dipolar reorientation of acetone molecules in an amorphous solid film under an external electric field. This paper is the first in a series of two papers investigating the effects of applied electric field on frozen molecular films. The other paper (referred to as Paper II[19]) immediately follows this one and examines the vibrational Stark effect of water molecules in ice crystals.

2. EXPERIMENTAL METHODS

All the experiments were conducted in an ultra-high-vacuum (UHV) chamber,[20] equipped with instrumentation for reflection absorption infrared spectroscopy (RAIRS), temperature-programmed desorption (TPD) mass spectrometry, and work function measurements, with the background pressure below 1×10^{-10} Torr (Figure 1). A frozen molecular film was

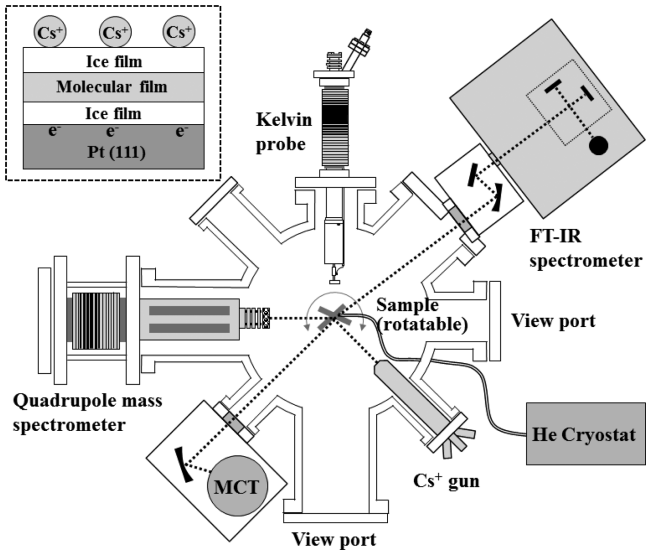

Figure 1. Schematic of the experimental apparatus. A molecular film was condensed onto a Pt(111) crystal, which is located at the chamber center and maintained at low temperature by a liquid He cryostat. The molecular film was covered with an ice overlayer and subsequently charged by depositing Cs^+ ions on the ice surface (see inset). The Kelvin work-function probe measured the voltage developed across the charged sample. The FT-IR spectrometer measured the molecular composition and orientation of the molecules in the sample. All the experiments were conducted under a UHV environment.

deposited on a Pt(111) single crystal surface maintained at a low temperature (~75 K) inside the UHV chamber. The Pt(111) surface was precleaned using sputtering and annealing procedures, and its cleanliness was verified from the TPD profile of the H_2O monolayer formed on the surface.[21] The temperature of the Pt(111) crystal was variable in the range of 70−1200 K and was monitored with an N-type thermocouple wire attached to the crystal.

Acetone or D_2O liquid was purified using freeze−vacuum−thaw cycles. Purity of the liquid samples was checked by introducing the vapors of the samples into the chamber through a leak valve and analyzing it with a quadrupole mass spectrometer. Acetone vapor was guided close to the Pt(111) substrate surface by a tube doser and deposited at a rate slower than 0.15 ML·s^{-1} (monolayer per second). The D_2O film was deposited using a backfilling method with a deposition rate below 0.16 ML·s^{-1}. The thicknesses of the molecular films were estimated from TPD measurements. The thickness of the D_2O film was determined by comparing its TPD intensity with that of a D_2O monolayer on Pt(111).[22] The thickness of the acetone film was calculated using the unit cell volume of the acetone crystal.[23] The film thicknesses are expressed in units of ML in this paper, where 1 ML represents 1.1×10^{15} molecules cm^{-2} for D_2O and 4.8×10^{14} molecules cm^{-2} for acetone.

Electric field was applied across the frozen molecular films using the ice film capacitor method, which was described in detail in a previous paper.[18] In this method, low-energy Cs^+ ions produced from a Cs^+ gun are sprayed onto the surface of a D_2O overlayer. The deposited Cs^+ ions float on the surface, owing to its thermodynamic affinity for the ice surface,[16,24] and induce an equivalent negative charge on the metal substrate surface underneath the molecular film. This charging phenomenon can be described like a charged parallel-plate capacitor. The electric field strength (F) within the charged molecular film can be expressed as $F = V/d = \sigma/\varepsilon_r\varepsilon_0$, where V is the voltage across the film, σ is the surface density of Cs^+ ions, d is the film thickness, ε_r is the relative permittivity of the film, and ε_0 is the vacuum permittivity. The film voltage was monitored by a Kelvin work-function probe,[15−17] which measured the difference in contact potential (ΔCPD) of the film before and after Cs^+ deposition. Samples composed of multiple stacks of acetone and D_2O were used in the present experiments. In this case, with different dielectric materials, the electric field strength within the acetone film can be expressed by eq 1.[18]

$$F(\text{acetone}) = \Delta\text{CPD}/[d(\text{acetone}) + d(\text{D}_2\text{O})\varepsilon_r(\text{acetone})/\varepsilon_r(\text{D}_2\text{O})] \quad (1)$$

In the above equation, ΔCPD is the voltage across the whole film, d (D_2O) and d (acetone) are the thicknesses of D_2O and acetone films, respectively, and ε_r (D_2O) and ε_r (acetone) are their dielectric constants. Since ε_r for solid acetone is unknown, we estimated ε_r (acetone) by assuming that the ε_r (D_2O)/ε_r (acetone) ratio is equal to the high-frequency relative permittivity (ε_∞) ratio of the corresponding liquids (i.e., ε_r (D_2O)/ε_r (acetone) = ε_∞ (D_2O)/ε_∞ (acetone) = 4.57/2 = 2.29).[25]

RAIRS measurements were performed in grazing angle (84°) reflection geometry[21,26] using a Fourier-transform infrared (FT-IR) spectrometer (PerkinElmer) with a mercury−cadmium telluride detector. The incident IR beam was linearly p-polarized using a wire grid polarizer (Edmund Optics). The beam path outside the UHV chamber was purged with dry nitrogen gas. RAIR spectra were averaged 256 times at a spectral resolution of 4 cm^{-1}.

3. RESULTS

To study the effect of electric field on amorphous solid acetone, we prepared samples in which the amorphous solid acetone film was sandwiched between two amorphous solid D_2O (D_2O−ASW) films. To prepare the samples, a ~46-ML-thick D_2O−ASW film was grown on a Pt(111) substrate at 75 K, following which a ~14-ML-thick acetone film was grown over the ASW film at the same temperature. Then, another ~46-ML-thick D_2O−ASW film was overlaid on the acetone film, thereby forming a D_2O-sandwiched acetone sample. An electric

DOI: 10.1021/acs.jpcc.5b01849
J. Phys. Chem. C 2015, 119, 15588−15595

field was applied across the sample by soft-landing Cs^+ ions onto the upper D_2O film surface.

The RAIR spectrum (a) in Figure 2 shows acetone absorbance bands measured before the electric field was

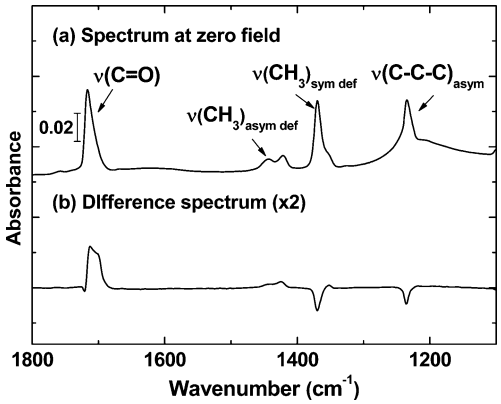

Figure 2. RAIR spectra showing the vibrational bands of amorphous solid acetone in an ASW-sandwiched acetone film [D_2O (46 ML)/acetone (14 ML)/D_2O (46 ML)/Pt(111)]. (a) Absorbance spectrum in the absence of applied electric field. (b) Field-on minus field-off difference spectrum, which shows the absorbance difference (ΔA) of the sample at the applied field strength of 4.3×10^8 V·m^{-1} and zero field. The difference spectrum is shown in a ×2 magnified scale.

applied. The shape and intensity ratios of the bands are characteristic of amorphous solid acetone,[27] indicating that the acetone film grown at 75 K had an amorphous structure with isotropic molecular distribution. In the same figure, spectrum (b) corresponds to the difference in the absorbance (ΔA) of the sample measured in the presence and absence of an applied field with a strength of 4.3×10^8 V·m^{-1}. All the measurements were conducted at 75 K, unless specified otherwise. The difference spectrum showed that the applied field increased the absorbance of the C═O stretching [ν(C═O)] and asymmetric methyl deformation [$\nu(CH_3)_{asym\ def}$] bands. On the other hand, the absorbance of asymmetric C−C−C stretching [$\nu(C-C-C)_{asym}$] and symmetric methyl deformation [$\nu(CH_3)_{sym\ def}$] bands decreased under the field.

RAIRS detects vibrations with transition dipole moment components parallel to the p-polarization of light, i.e., perpendicular to the Pt(111) surface. Therefore, the absorbance changes in Figure 2 indicate that acetone molecules that were initially randomly orientated in the amorphous solid were reoriented by the applied field. Although the ratio of the RAIR band intensities changed with applied field, the TPD experiments revealed that the total amount of acetone in the sample remained unchanged due to the application of electric field.

Next, the electric field strength was increased from zero to 4.3×10^8 V·m^{-1} in four stages by depositing increasing amounts of Cs^+ ions on the sample surface, and the absorbance of the various acetone vibrational bands at different field strengths is shown in Figure 3. The field strength was estimated by Kelvin probe measurements after each stage of Cs^+ deposition. Figure 3 clearly shows that the ν(C═O) band intensity increased, whereas the $\nu(C-C-C)_{asym}$ and $\nu(CH_3)_{sym\ def}$ band intensities decreased with increasing field strength. Note that the direction of the transition dipole moment of ν(C═O) is different from those of $\nu(C-C-C)_{asym}$ or $\nu(CH_3)_{sym\ def}$ (see Figure A2). Since the intensity of the

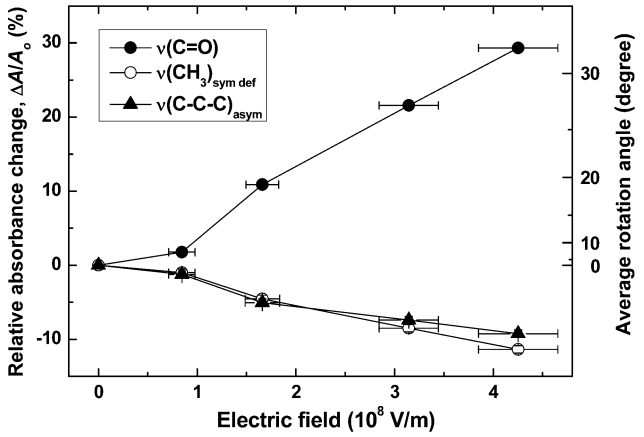

Figure 3. Variation in the absorbance of acetone vibrational bands as a function of applied field strength. $\Delta A/A_0$ on the left ordinate indicates the relative change in absorbance, i.e., the field-on (A) minus the field-off (A_0) absorbances, divided by the field-off absorbance. The average rotation angle indicated on the right ordinate indicates the extent of dipole alignment along the field and is estimated from the $\Delta A/A_0$ data for the ν(C═O) band. Additional explanation is provided in Section 4A.

RAIR bands depends on the angle between the p-polarization of light and the direction of transition dipole moment, according to the Fermi golden rule, the result indicates that the applied electric field reorients acetone molecules such that the C═O bond becomes parallel to the field, whereas the $\nu(C-C-C)_{asym}$ and $\nu(CH_3)_{sym\ def}$ vibrations become perpendicular to the field.

At the field strength of 4.3×10^8 V·m^{-1}, the relative absorbance of ν(C═O) increased by 29%, whereas those of $\nu(C-C-C)_{asym}$ and $\nu(CH_3)_{sym\ def}$ decreased by 9% and 11%, respectively. These absorbance changes correspond to the rotation of acetone molecules by an average angle of 31°, as estimated using a molecular geometry model, which will be discussed in Section 4A.

In the next experiment, we examined the effect of increasing or decreasing the electric field strength on the RAIRS spectrum. The series of spectra shown at the top in Figure 4 (denoted by (a)) are the difference spectra obtained as the electric field strength was increased from zero to 4.3×10^8 V·m^{-1}. The difference spectra show that a stronger applied field produced a greater change in the band intensities.

The series of spectra shown at the bottom of Figure 4 (denoted by (b)) are the difference spectra obtained as the electric field was decreased from 4.3×10^8 to 2.2×10^8 V·m^{-1} and further to 1.4×10^8 V·m^{-1}. The applied field was reduced by spraying low-energy (~10 eV) electrons onto the ASW film surface of the sample, which was originally positively charged after Cs^+ deposition. According to recent studies,[17] low-energy electrons tend to accumulate predominantly on the surface of ASW films. The Kelvin probe was used to measure the film voltage after each stage of electron exposure. The difference spectra showed that decreasing the field strength did not restore the band intensities fully to their initial values. In particular, the band intensities of $\nu(C-C-C)_{asym}$, $\nu(CH_3)_{sym\ def}$, and $\nu(CH_3)_{asym\ def}$ were changed only slightly by the decrease in the field intensities. In contrast, the ν(C═O) band was more distinctly changed by the decrease in the electric field compared to the other bands. However, it may be

DOI: 10.1021/acs.jpcc.5b01849
J. Phys. Chem. C 2015, 119, 15588−15595

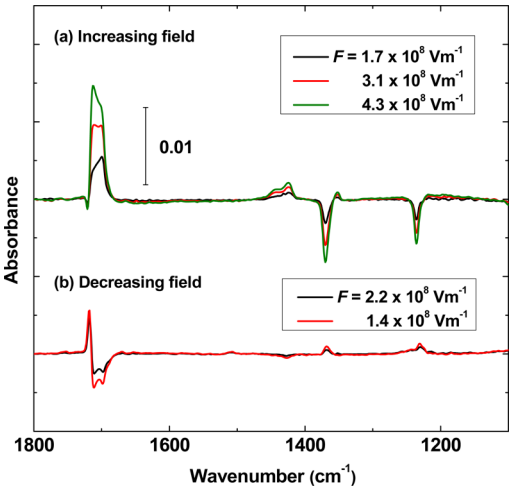

Figure 4. Change in the acetone bands during progressive increase and decrease in the applied electric field strength. (a) Series of difference spectra as the field strength is increased from zero to 4.3×10^8 V·m^{-1}. Baseline subtraction was made with respect to the zero-field spectrum to yield the difference spectra. (b) Difference spectra obtained as the field strength is decreased from 4.3×10^8 to 2.2×10^8 V·m^{-1} and further to 1.4×10^8 V·m^{-1}. In this case, baseline subtraction was made against the absorbance spectrum at the highest field (4.3×10^8 V·m^{-1}) to yield the difference spectra. The sample structure was D_2O (46 ML)/acetone (14 ML)/D_2O (46 ML)/Pt(111).

noted that it was mostly the shape of the ν(C═O) band that was changed, rather than its net absorption intensity.

The fact that the $\nu(C-C-C)_{asym}$, $\nu(CH_3)_{sym\ def}$, and $\nu(CH_3)_{asym\ def}$ band intensities are not fully restored by the decrease in the field strength indicates the irreversible nature of the dipolar reorientation in amorphous solid acetone. A stronger field induces a greater degree of dipole alignment in the solid. However, once dipolar polarization occurs, decreasing the field strength does not easily restore the original isotropic configuration. The irreversible polarization and depolarization behaviors of amorphous solid acetone contrast with the behaviors of polar liquids, in which case the dipolar equilibrium shifts reversibly with applied field. Obviously, the difference can be attributed to the fact that molecular motion is restricted in amorphous solids at low temperatures, and the energy barrier for reorientation is very large compared to the thermal energy available.

It is also worth mentioning that a crystalline acetone sample prepared by annealing an amorphous acetone sample at 140 K,[27] exhibited negligible change in the band intensities under an electric field of comparable strength (data not shown). This observation indicated that molecular reorientation was more difficult in a crystalline solid than in an amorphous solid, owing to stronger intermolecular attractions in the former case.

In Figure 4, it can be seen that a change in the electric field strength significantly changed the shape of the ν(C═O) band as well as its intensity. During the initial increase in the field strength (spectral series (a)), the ν(C═O) band intensity increased more strongly in the low frequency region (~1699 cm^{-1}) than in the high frequency region (~1708 cm^{-1}). However, as the field became stronger (e.g., at 4.3×10^8 V·m^{-1}), the band intensity increased significantly in the high frequency region at 1708 cm^{-1}. According to previous RAIRS studies on acetone solids,[27] the 1699 cm^{-1} component of the band is assigned to "interfacial" acetone molecules, which most likely correspond to the molecules in the acetone−water boundary regions of the sample, whereas the 1708 cm^{-1} band is attributed to the "bulk" acetone molecules in the interior of the sample. Therefore, the present results suggest that the interfacial acetone molecules reorient more easily than the bulk molecules under applied electric field.

To further investigate this hypothesis, we studied acetone samples with different structures, including a "bulk-dominant" sample with a relatively thick (~14 ML) acetone film sandwiched between ASW films, and an "interface-dominant" sample where the same total amount of acetone as the "bulk-dominant" sample was divided into three thin (~5 ML) layers stacked alternately with ASW films. Figure 5 shows the field-on

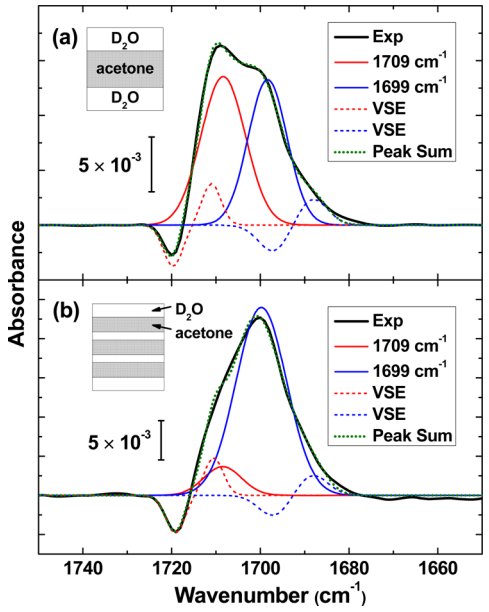

Figure 5. Difference spectra of the ν(C═O) band measured at a field strength of 4×10^8 V·m^{-1} shown in high resolution. (a) "Bulk-dominant" sample containing a single acetone film [D_2O (46 ML)/acetone (14 ML)/D_2O (46 ML)/Pt(111)]. (b) "Interface-dominant" sample containing three thin acetone films [D_2O (40 ML)/acetone (5 ML)/D_2O (26 ML)/acetone (5 ML)/D_2O (26 ML)/acetone (5 ML)/D_2O (35 ML)/Pt(111)]. The result of the multiple-peak analysis is also shown overlapped with the sample spectra. The various components of the spectra are explained in Section 4B.

minus field-off difference spectra for the ν(C═O) band measured for these samples, with an applied field strength of 4×10^8 V·m^{-1}. For the "bulk-dominant" sample (Figure 5a), the ν(C═O) band intensity significantly increased at both ~1699 cm^{-1} and ~1708 cm^{-1} under applied field. On the other hand, for the "interface-dominant" sample (Figure 5b), the band intensity increased mostly at ~1699 cm^{-1}. These differences support the hypothesis that the 1699 cm^{-1} component corresponds to acetone molecules in the interfacial region. In addition, a small decrease in the ν(C═O) band intensity at ~1720 cm^{-1} was observed and discussions on this feature will be reserved for Section 4B.

4. DISCUSSION

4A. Extent of Dipolar Polarization. The trends observed in the ν(C═O), $\nu(C-C-C)_{asym}$, $\nu(CH_3)_{sym\ def}$, and $\nu(CH_3)_{asym\ def}$ band intensities with increase in the electric field strength, shown in Figures 3 and 4, indicate that dipolar

DOI: 10.1021/acs.jpcc.5b01849
J. Phys. Chem. C 2015, 119, 15588−15595

reorientation of acetone occurs along the field direction. To estimate the degree of reorientation, the field-dependent band intensities can be analyzed using a molecular geometry model. To perform this analysis, we first need to determine a quantitative relationship between the RAIR band intensity and molecular orientation. Figure A1 in the Appendix illustrates the molecular orientation and angles defined in the model. According to the Fermi golden rule, the magnitude of the transition matrix element in RAIRS is proportional to the cosine of the angle (θ) between the p-polarization of light and the direction of the transition dipole moment. In addition, the transition probability is proportional to the square of the transition matrix element of an oscillator.[28] Therefore, the RAIRS absorbance is proportional to the square of cosine of the angle θ (i.e., $A \propto \cos^2 \theta$).

To simulate the absorbance change (ΔA) due to molecular reorientation, we use a simplifying assumption that all the acetone molecules in the sample are reoriented by the same angle ($\Delta\theta$) under a given field strength. Molecules whose initial dipole direction (θ_0) is very close to the field direction such that $\theta_0 < \Delta\theta$ are exempted from this assumption. These molecules are tilted only up to the field direction and their tilt angle is equal to θ_0. With this simplification, an ensemble of molecular reorientations can be expressed by a single variable $\Delta\theta$, which may be regarded as the average rotation angle of the acetone molecules under applied field. The experimentally measured ΔA values correspond to the difference in absorbance before and after the dipole polarization of a sample. To simulate ΔA, the absorbance (A_0) of an isotropic sample under zero field is first calculated using a set of acetone molecules. The molecules are then tilted by $\Delta\theta$, as mentioned above, and the absorbance of the tilted molecular ensemble is calculated. Further detail is described in Appendix A. Figure A2 shows the simulated relative absorbance change ($\Delta A/A_0$) curves for the different molecular vibrations as a function of $\Delta\theta$.

By comparing the experimental results shown in Figure 3 with the theoretical $\Delta A/A_0$ curves (Figure A2), the average rotation angle of molecules in the sample under a given field strength can be deduced. For example, the experimental value of $\Delta A/A_0$ for ν(C═O) at a field strength of 4.3×10^8 V·m^{-1} was 29%. This corresponds to $\Delta\theta$ of about 31° on the theoretical curve of $\Delta A/A_0$ versus $\Delta\theta$ for α (angle of transition dipole moment) = 0°, which corresponds to the ν(C═O) vibration. The theoretical $\Delta A/A_0$ values for the other vibrations can be predicted in a straightforward manner if the value of α for these vibrations relative to the direction of the C═O vibration is known. However, the transition dipole moment angle of these vibrations is not clearly known due to the effect of intermolecular vibrational coupling in the solid.[29] We may assume that the vibrations in amorphous solids resemble either the normal mode vibrations of free molecules or local mode vibrations, although the real situation may be somewhere between these two extreme assumptions. If we use the normal mode approximation, the transition dipole moment direction of $\nu(C-C-C)_{asym}$ and $\nu(CH_3)_{sym\ def}$ will be 90° with respect to the ν(C═O) direction. On the other hand, if we make the local mode approximation, the corresponding ν(C−C) and $\nu(CH_3)_{def}$ vibrations will have an angle of 120° with respect to ν(C═O). The $\Delta A/A_0$ curves for the two cases (α = 90° and 120°) are plotted in Figure A2. These curves may be compared with the experimental data shown in Figure 3 to estimate the average rotation angle of acetone. The experimental $\nu(C-C-C)_{asym}$ and $\nu(CH_3)_{sym\ def}$ data shown in Figure 3 correspond to $\Delta\theta$ = 26−28° at the field strength of 4.3×10^8 V·m^{-1} with the normal mode approximation. The same data yields $\Delta\theta$ = 55−59° with the local mode approximation. It may be noted that the $\Delta\theta$ value obtained with the normal mode approximation is closer to the value obtained from the ν(C═O) data ($\Delta\theta \approx$ 31°).

The analyses indicate that a substantial degree of molecular reorientation occurs in the presence of electric field. An order-of-magnitude calculation shows that the electrostatic energy of dipole flipping under the field ($E = \mu F/\varepsilon_r$) is ∼2 kJ·mol^{-1}, where $\mu = 9.77 \times 10^{-30}$ C·m, $\varepsilon_r \sim 1$ for solid acetone, and the applied field $F = 4 \times 10^8$ V·m^{-1}. Because this dipole energy is larger than the thermal energy at 75 K, the acetone molecules can be reoriented by the field, unless the reorientational motion has a large energy barrier. It will be interesting to do theoretical study of the reorientation dynamics of amorphous solid acetone under electric field to compare with the experimental observation.

The acetone band intensities change irreversibly as the electric field strength is increased or decreased, as mentioned in Figure 4. As the field strength is decreased, the intensities and shapes of the $\nu(C-C-C)_{asym}$, $\nu(CH_3)_{sym\ def}$, and $\nu(CH_3)_{asym\ def}$ bands do not change significantly (Figure 4b). However, the ν(C═O) band changes in a peculiar way. A decrease in the field strength results in a decrease in the ν(C═O) absorbance in the low frequency region, whereas the absorbance in the high-frequency region increases simultaneously. In general, molecular reorientation results in either a net increase or decrease in the absorbance of the vibrational band. Therefore, for interpreting the ν(C═O) spectral behavior in relation to the molecular reorientation, the simultaneously increasing and decreasing portions of the ν(C═O) band may be canceled out. The absorbance change that remains after the simultaneously increasing and decreasing portions are removed from the ν(C═O) spectrum will represent the effect of the reorientation of acetone molecules. The absorbance change calculated in this manner for the ν(C═O) band as the field is decreased from 4.3×10^8 to 1.4×10^8 V·m^{-1} is about 19% of the absorbance change that appears for the field increase from zero to 4.3×10^8 V·m^{-1}. This value of 19% indicates the degree of depolarization of the sample as the field strength is decreased. The depolarization degree can be deduced from other acetone bands as well, and are estimated to be about 11% and 17% from the $\nu(CH_3)_{sym\ def}$ and $\nu(C-C-C)_{asym}$ bands, respectively, for the same decrease in field strength (from 4.3×10^8 to 1.4×10^8 V·m^{-1}). The values calculated from the three bands are in reasonable agreement with each other and indicate only a small degree of depolarization. The result further supports the conclusions regarding the irreversible nature of dipole reorientation under applied field.

4B. Multiple-Peak Analysis of the ν(C═O) Band. The changes in the spectral shape of the ν(C═O) band with electric field, shown in Figures 4 and 5, suggest that acetone molecules in the interfacial region (corresponding to the 1699 cm^{-1} peak) are more easily aligned along the field direction than the molecules in the bulk phase (1708 cm^{-1}). We performed multiple-peak analysis for the ν(C═O) difference spectra to examine the field-dependent changes in more detail, the result of which is shown overlapped with the spectra in Figure 5. In Figure 5a, it can be seen that most of the increase in absorbance for the ν(C═O) band under applied field can be explained by the increases in the ∼1699 cm^{-1} and ∼1709 cm^{-1} components. In this analysis, the bulk acetone peak is located at

DOI: 10.1021/acs.jpcc.5b01849
J. Phys. Chem. C 2015, 119, 15588−15595

1709 cm^{-1} rather than at 1708 cm^{-1} as assigned in the previous work,[27] to achieve a better fit. However, this amount of difference is not physically meaningful. For the "interface-dominant" sample, shown in Figure 5b, the absorbance primarily increases for the 1699 cm^{-1} component, which is assigned to acetone molecules that are H-bonded with water at the acetone/water interface.[30,31] The spectral analysis shows that the acetone molecules at the interface are tilted more easily under applied field. It could be imagined that the applied field works synergistically with the acetone−water H-bonding interactions to reorient the molecules. However, more recent studies[27] show that the peak at 1699 cm^{-1} is not necessarily due to the H-bonded species. Instead, it may just be due to the weakly bonded acetone molecules at the interface, because this peak appears even for an acetone film grown on a pure metal surface. Therefore, we may conclude that the interfacial acetone molecules are easily reoriented by the applied field regardless of the formation of hydrogen bonds.

A peculiar feature in the ν(C═O) spectra of Figure 4a and Figure 5 is the dip appearing at ∼1720 cm^{-1} as the field strength is increased. The dip transforms into a peak as the field strength is decreased (Figure 4). These phenomena may be interpreted as indications of the removal or appearance of the 1720 cm^{-1} component in the sample as the field strength is increased or decreased, respectively. However, this frequency is unusually high for the ν(C═O) band of acetone and a peak at this frequency has never been observed for solid acetone at zero field. Crystalline acetone has a peak at a close, but easily distinguishable position (1717 cm^{-1}).[27] Moreover, crystalline acetone does not undergo dipolar polarization under these field conditions. Further, the spectral fitting was unsatisfactory with this component included in the low frequency region of the ν(C═O) band. For these reasons, the possibility of the existence of a species corresponding to the peak at 1720 cm^{-1} in the solid acetone sample must be discarded.

The absorbance change at ∼1720 cm^{-1} may be explained in terms of the vibrational Stark shift of ν(C═O). Normally, the Stark effect appears as band broadening for an amorphous solid sample, owing to the ensemble average of randomly distributed chromophores[10,11,19]). However, the Stark effect can also appear as a frequency shift for molecularly aligned samples like in the present case. When the C═O dipole of acetone is aligned toward the field, the Stark effect will produce a red shift in the ν(C═O) frequency.[13] This shift will appear as a dip in the high-frequency edge of the ν(C═O) band in the difference spectrum, and the absorbance will increase by the same amount in the low-frequency edge. The experimental observations agree with this expectation. Indeed, accounting for the Stark shift for the ∼1699 and ∼1709 cm^{-1} components (the dashed curves in blue and red, respectively) in the multiple-peak analysis significantly improved the quality of the spectral fitting, as shown in Figure 5, where the green dotted curve indicates the simulated curve with the Stark shift included. Here, the Stark effect was simulated by using adjustable parameters for the frequency shift and band broadening to optimize the spectral fitting. Nonetheless, the reasonably satisfactory fitting achieved by this approach, and the fact that the absorbance at ∼1720 cm^{-1} changes reversibly with field strength, support the interpretation that this feature originates from the vibrational Stark shift of the ν(C═O) band.

5. SUMMARY

We have examined the changes in the IR spectra of amorphous solid acetone under the influence of strong electric fields by conducting RAIRS measurements on samples located within the ice film capacitor. The shape and intensity changes of the acetone vibrational bands provide information regarding the structural changes of the sample under applied field. To the best of our knowledge, this work is the first observation of dipolar reorientation of small molecules with IR spectroscopy under well-controlled electric field conditions. The observation can be summarized as follows.

1. The acetone molecules are dipole-reoriented along the field direction. The degree of dipolar polarization increases as the field strength is increased in the range of $(0.8-4.3) \times 10^8$ $V \cdot m^{-1}$, reaching a molecular tilt angle of about 31° on average at the highest field strength (4.3×10^8 $V \cdot m^{-1}$).

2. The molecular reorientation occurs irreversibly as the field strength is increased or decreased for amorphous solid acetone. This behavior contrasts with the reversible dipolar equilibrium of polar liquids under applied field. For crystalline acetone at 75 K, molecular reorientation does not occur to any appreciable degree at comparable field strengths.

3. Multiple-peak analyses of the ν(C═O) spectra reveal that the acetone molecules in the interfacial region are reoriented more easily compared to those in the bulk.

APPENDIX

Molecular Geometry Model for the Simulation of RAIRS Absorbance Change Due to Dipole Reorientation

The model comprises a set of acetone molecules, which have an isotropic molecular orientation in the absence of externally applied electric field. The angle between the direction of p-polarization of light and the transition dipole moment of molecules is expressed by a set of angles, $X_{iso} = (\theta_{iso,1}, \theta_{iso,2}, ..., \theta_{iso,n})$. The p-polarization direction of light is equal to the direction of the applied electric field in the present experiment. The model uses a simplifying assumption that all acetone molecules are reoriented by the same amount of angle ($\Delta\theta$) at a given electric field strength. Molecules whose initial dipole direction (θ_0) is close to the field direction ($\theta_0 < \Delta\theta$) are exempted from this assumption. These pre-aligned molecules can be tilted only up to the field direction, i.e., $\Delta\theta = \theta_0$. The reoriented configuration of molecules under the field is denoted by a set of new angles, $X_{tilt} = (\theta_{tilt,1}, \theta_{tilt,2},..., \theta_{tilt,n}) = (\theta_{iso,1} - \Delta\theta, \theta_{iso,2} - \Delta\theta, ..., \theta_{iso,n} - \Delta\theta)$. The absorbance change due to an applied field is the absorbance difference between a set of reoriented molecules and a set of isotropic molecules. The absorbance of a vibrational band in RAIRS is proportional to $\cos^2\theta$ (section 4A). Therefore, the relative absorbance change is expressed by eq A1.

$$\Delta A/A_0 = \frac{A - A_0}{A_0} = \frac{\sum_n \cos^2\theta_{tilt} - \sum_n \cos^2\theta_{iso}}{\sum_n \cos^2\theta_{iso}} \quad \text{(A1)}$$

Under the influence of electric field, the C═O axis of acetone is inclined towards the field direction. In the following analysis, we denote the direction of the C═O bond with respect to the direction of p-polarization of light as the principal angle (θ). The angle of the transition dipole moment of the other vibrations with respect to the C═O direction is denoted by α (Figure A1). Computed values of the relative absorbance change ($\Delta A/A_0$) are plotted as a function of the average

DOI: 10.1021/acs.jpcc.5b01849
J. Phys. Chem. C 2015, 119, 15588−15595

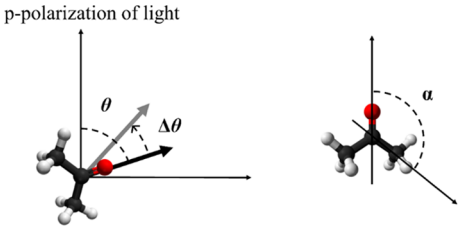

Figure A1. Illustration of the angles and molecular geometry used in the model. θ indicates the angle between the p-polarization of light and the direction of transition dipole moment of C═O vibration. α is a molecular internal angle indicating the direction of a different vibration mode with respect to the C═O vibration.

rotation angle in Figure A2. The curves are shown for α = 0°, 90°, and 120°. If all the acetone molecules are perfectly aligned

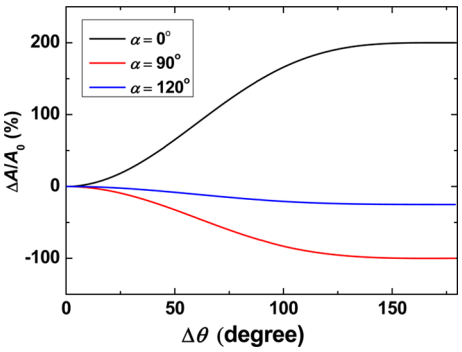

Figure A2. Computed curves of the relative absorbance change ($\Delta A/A_0$) versus the average rotation angle ($\Delta\theta$). The α = 0° curve corresponds to ν(C═O). The α = 90° curve simulates ν(C−C−C)$_{asym}$ and $\nu(CH_3)_{sym\ def}$ in the normal mode approximation, and the α = 120° curve simulates ν(C−C) and $\nu(CH_3)_{def}$ in the local mode approximation.

along the field direction, which corresponds to $\Delta\theta$ = 180° in the plot, then the relative absorbance of ν(C═O) is increased by 200% from the isotropic value ($\Delta A/A_0$ = 200%). In this case, the absorbance of a vibrational mode with α = 90° is reduced to zero ($\Delta A/A_0$ = −100%).

AUTHOR INFORMATION

Corresponding Author

*E-mail: surfion@snu.ac.kr. Phone: +82-2-875-7471.

Notes

The authors declare no competing financial interest.

ACKNOWLEDGMENTS

This work was supported by Samsung Science and Technology Foundation (SSTF-BA1301-04).

REFERENCES

(1) Debye, P. Some Results of Kinetic Theory of Isolators. *Phys. Z.* **1912**, *13*, 97−100.
(2) Simons, R. Strong Electric-Field Effects on Proton-Transfer between Membrane-Bound Amines and Water. *Nature* **1979**, *280*, 824−826.
(3) Simons, R. Electric-Field Effects on Proton-Transfer between Ionizable Groups and Water in Ion-Exchange Membranes. *Electrochim. Acta* **1984**, *29*, 151−158.
(4) Onsager, L. Deviations from Ohm's Law in Weak Electrolytes. *J. Chem. Phys.* **1934**, *2*, 599.
(5) Toney, M. F.; Howard, J. N.; Richer, J.; Borges, G. L.; Gordon, J. G.; Melroy, O. R.; Wiesler, D. G.; Yee, D.; Sorensen, L. B. Voltage-Dependent Ordering of Water-Molecules at an Electrode-Electrolyte Interface. *Nature* **1994**, *368*, 444−446.
(6) Weaver, M. J.; Gao, X. In-Situ Electrochemical Surface Science. *Annu. Rev. Phys. Chem.* **1993**, *44*, 459−494.
(7) Ataka, K.; Yotsuyanagi, T.; Osawa, M. Potential-Dependent Reorientation of Water Molecules at an Electrode/Electrolyte Interface Studied by Surface-Enhanced Infrared Absorption Spectroscopy. *J. Phys. Chem.* **1996**, *100*, 10664−10672.
(8) Honig, B. H.; Hubbell, W. L.; Flewelling, R. F. Electrostatic Interactions in Membranes and Proteins. *Annu. Rev. Biophys. Biophys. Chem.* **1986**, *15*, 163−193.
(9) Nakamura, H. Roles of Electrostatic Interaction in Proteins. *Q. Rev. Biophys.* **1996**, *29*, 1−90.
(10) Bublitz, G. U.; Boxer, S. G. Stark Spectroscopy: Applications in Chemistry, Biology, and Materials Science. *Annu. Rev. Phys. Chem.* **1997**, *48*, 213−242.
(11) Boxer, S. G. Stark Realities. *J. Phys. Chem. B* **2009**, *113*, 2972−2983.
(12) Labhart, H. Electrochromism. *Adv. Chem. Phys.* **1967**, *13*, 179.
(13) Lambert, D. K. Vibrational Stark-Effect of CO on Ni(100), and CO in the Aqueous Double Layer: Experiment, Theory, and Models. *J. Chem. Phys.* **1988**, *89*, 3847−3860.
(14) Stuve, E. M. Ionization of Water in Interfacial Electric Fields: An Electrochemical View. *Chem. Phys. Lett.* **2012**, *519*, 1−17.
(15) Lilach, Y.; Iedema, M. J.; Cowin, J. P. Proton Segregation on a Growing Ice Interface. *Surf. Sci.* **2008**, *602*, 2886−2893.
(16) Tsekouras, A. A.; Iedema, M. J.; Cowin, J. P. Amorphous Water-Ice Relaxations Measured with Soft-Landed Ions. *Phys. Rev. Lett.* **1998**, *80*, 5798−5801.
(17) Horowitz, Y.; Asscher, M. Low Energy Charged Particles Interacting with Amorphous Solid Water Layers. *J. Chem. Phys.* **2012**, *136*, 134701.
(18) Shin, S.; Kim, Y.; Moon, E.-s.; Lee, D. H.; Kang, H.; Kang, H. Generation of Strong Electric Fields in an Ice Film Capacitor. *J. Chem. Phys.* **2013**, *139*, 074201.
(19) Shin, S.; Kang, H.; Cho, D.; Lee, J. Y.; Kang, H. Effect of Electric Field on Condensed-Phase Molecular Systems. II. Stark Effect on the Hydroxyl Stretch Vibration of Ice. *J. Phys. Chem C* **2015**, DOI: 10.1021/acs.jpcc.5b01850.
(20) Kang, H. Reactive Ion Scattering of Low Energy Cs^+ from Surfaces. A Technique for Surface Molecular Analysis. *Bull. Korean Chem. Soc.* **2011**, *32*, 389−398.
(21) Haq, S.; Harnett, J.; Hodgson, A. Growth of Thin Crystalline Ice Films on Pt(111). *Surf. Sci.* **2002**, *505*, 171−182.
(22) Hodgson, A.; Haq, S. Water Adsorption and the Wetting of Metal Surfaces. *Surf. Sci. Rep.* **2009**, *64*, 381−451.
(23) Allan, D.; Clark, S.; Ibberson, R.; Pulham, C. The Influence of Pressure and Temperature on the Crystal Structure of Acetone. *Chem. Commun.* **1999**, 751−752.
(24) Moon, E.-s.; Kim, Y.; Shin, S.; Kang, H. Asymmetric Transport Efficiencies of Positive and Negative Ion Defects in Amorphous Ice. *Phys. Rev. Lett.* **2012**, *108*, 226103.
(25) Barthel, J.; Buchner, R. High Frequency Permittivity and Its Use in the Investigation of Solution Properties. *Pure Appl. Chem.* **1991**, *63*, 1473−1482.
(26) Marchand, P.; Marcotte, G.; Ayotte, P. Spectroscopic Study of HNO_3 Dissociation on Ice. *J. Phys. Chem. A* **2012**, *116*, 12112−12122.
(27) Shin, S.; Kang, H.-I.; Kim, J. S.; Kang, H. Phase Transitions of Amorphous Solid Acetone in Confined Geometry Investigated by Reflection Absorption Infrared Spectroscopy. *J. Phys. Chem. B* **2014**, *118*, 13349−13356.
(28) Craig, D. P.; Thirunamachandran, T. *Molecular Quantum Electrodynamics: an Introduction to Radiation-Molecule Interactions*; Academic Press: London, 1984.
(29) Shi, L.; Gruenbaum, S. M.; Skinner, J. L. Interpretation of IR and Raman Line Shapes for H_2O and D_2O Ice Ih. *J. Phys. Chem. B* **2012**, *116*, 13821−13830.

DOI: 10.1021/acs.jpcc.5b01849
J. Phys. Chem. C 2015, 119, 15588−15595

(30) Schaff, J. E.; Roberts, J. T. Structure Sensitivity in the Surface Chemistry of Ice: Acetone Adsorption on Amorphous and Crystalline Ice Films. *J. Phys. Chem.* **1994**, *98*, 6900−6902.
(31) Schaff, J. E.; Roberts, J. T. The Adsorption of Acetone on Thin Films of Amorphous and Crystalline Ice. *Langmuir* **1998**, *14*, 1478−1486.

DOI: 10.1021/acs.jpcc.5b01849
J. Phys. Chem. C 2015, 119, 15588−15595